

Article

Effect of Mo and C Additions on Eta Phase Evolution of WC-13Co Cemented Carbides

Xun Li ¹, Xianwei Zhang ², Junfei Zhang ², Qiang Zhang ², Vincent Ji ³ and Jinlong Liu ^{1,*}

¹ Key Laboratory for Anisotropy and Texture of Materials (Ministry of Education), School of Materials Science and Engineer, Northeastern University, Shenyang 110819, China

² Liaoning Wuhuan Special Materials and Intelligent Equipment Industry Technology Research Institute Co., Ltd., Shenyang 113122, China

³ Institut de Chimie Moléculaire et Des Matériaux d'Orsay, CNRS UMR 8182, Université Paris-Saclay, 91405 Orsay, France

* Correspondence: liujl@atm.neu.edu.cn; Tel.: +86-24-83681455; Fax: +86-24-83686455

Abstract: The WC-13Co (wt.%) cemented carbide was prepared by simple pressureless sintering, and the influence of Mo and C additions on the eta evolution and mechanical properties was analyzed by XRD, SEM, EDS, XPS, and Vickers hardness tester. The results show that the addition of Mo has an important influence on the composition, size, and distribution of the eta phase and Mo₂C phase. When the Mo content increases from 0 to 2.5%, the Mo-enriched eta phase grows abnormally and the area fraction of the eta phase significantly increases to 40%, leading to an obvious increase in hardness from 1232 HV₃₀ to 1321 HV₃₀, and a decrease in fracture toughness from 12.5 MPa·m^{1/2} to 9.8 MPa·m^{1/2}. The addition of carbon black effectively inhibits the formation of the eta phase in the samples with 2.5% Mo. Moreover, adding Mo can suppress WC coarsening in a high-carbon content, which is different from the obvious growth of WC grains in a high-carbon environment in traditional research. Finally, the mechanism of eta phase evolution during the sintering process of WC-Co cemented carbides containing Mo is discussed systematically.



Citation: Li, X.; Zhang, X.; Zhang, J.; Zhang, Q.; Ji, V.; Liu, J. Effect of Mo and C Additions on Eta Phase Evolution of WC-13Co Cemented Carbides. *Coatings* **2022**, *12*, 1993. <https://doi.org/10.3390/coatings12121993>

Academic Editor: Michał Kulka

Received: 31 October 2022

Accepted: 16 December 2022

Published: 19 December 2022

Publisher's Note: MDPI stays neutral with regard to jurisdictional claims in published maps and institutional affiliations.



Copyright: © 2022 by the authors. Licensee MDPI, Basel, Switzerland. This article is an open access article distributed under the terms and conditions of the Creative Commons Attribution (CC BY) license (<https://creativecommons.org/licenses/by/4.0/>).

Keywords: WC-Co; cemented carbide; eta phase; Mo

1. Introduction

The WC-Co cemented carbides consisting of WC grains coated by Co binders have excellent mechanical properties, including high hardness, high wear resistance, and favorable fracture toughness [1]. It is widely used in metal-cutting, mining, construction, and rock drilling [2]. Alloying is an effective method to improve the mechanical properties of WC-Co cemented carbides. Li et al. [3] found that Cu-doped WC-Co cemented carbides have excellent comprehensive performances. The average WC grain size decreases as Cu is added, and the grain size distribution narrows. The addition of Al can greatly improve the hardness and density of the WC-Co cemented carbides, but its fracture toughness decreases [4]. The addition of the Cr element promotes the segregation of the M₇C₃ phase around the eta phase, which can inhibit the growth of the eta phase, and leads to the finer and more dispersed eta phase [5].

Recently, some reports showed that the addition of Mo [6] or Mo₂C [7], which obviously enhanced the wettability between WC grains and binder phases, is beneficial to improving the mechanical properties of WC-Co cemented carbides. Some studies further indicated that hardness [8], fracture toughness [9], and bending strength increase with the addition of Mo in cemented carbide. Moreover, Guo et al. [10] also reported that Mo is helpful to improve the corrosion resistance of WC-6Co cemented carbide in both acidic and alkaline solutions.

In addition, the phase is a key factor in the mechanical properties of cemented carbides. Especially for high-temperature sintering, the phases in W-C-Co ternary phase diagram system are very complex, and the possible phases include eta phases (Co₆W₆C and Co₃W₃C),

ditungsten carbide (W_2C), and the intermediate Co_7W_6 phase [11]. However, the effect of Mo addition on the formation and growth of the phase is still very limited. The current work mainly focused on investigating the effect of Mo addition on the phase of WC-13Co cemented carbides, and the difference in microstructure evolution of WC-13Co cemented carbide containing Mo is further explored in the sintering environments of both low-carbon and high-carbon.

2. Experimental Procedure

Commercial tungsten carbides (5.92% C, 0.094% O, $W \geq 93.98$, $S \leq 0.001\%$, $P \leq 0.001\%$, others $\leq 0.001\%$, wt.%, average particle size of 1.5 μm , Xiamen golden egret special alloy Co., Ltd., Xiamen, China, Figure 1a), Co powders ($Co \geq 99.9\%$, $Mn \leq 0.0001\%$, $Cu \leq 0.0003\%$, others $\leq 0.005\%$, average particle size of 0.8 μm , 99.9 wt.% purity, Xiamen golden egret special alloy Co., Ltd., Xiamen, China, Figure 1b), Mo powders ($Mo \geq 99.0\%$, average particle size of 2 μm , Shanghai Macklin Biochemical Technology Co., Ltd., Shanghai, China, Figure 1c) were selected as raw materials. Table 1 shows the nominal chemical compositions of WC-13Co cemented carbides with different additives of Mo and carbon black. The carbon content of the sample is calculated using the following formula: $C_{total}\% = (C_{WC} + C_{carbon})/M_{total}$, where $C_{total}\%$ is the proportion of C in the sample, C_{WC} is the weight of C in the WC powder, C_{carbon} is the weight of carbon black added, and the M_{total} is the total weight of the sample. The C_{total} is important for evaluating the carbon content in the sample, although it ignores the carbon loss during the sintering process.

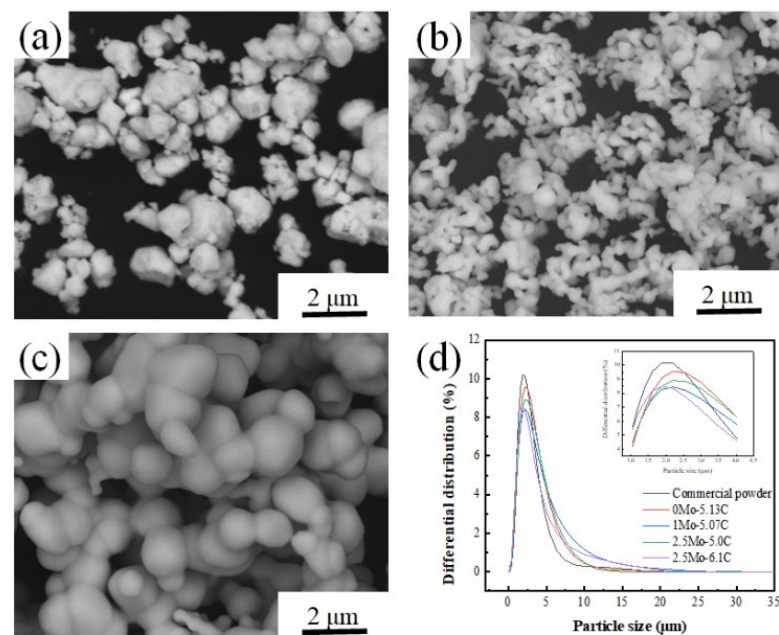


Figure 1. SEM of (a) WC powders, (b) Co powders, (c) Mo powders, (d) Size distribution of commercial WC and ball-milled powders.

Table 1. The nominal chemical compositions of WC-13Co cemented carbides (wt.%).

Samples	WC	Co	Mo	C	C_{total}
0Mo-5.13C	87	13	0	0	C5.13
1Mo-5.07C	86	13	1	0	C5.07
2Mo-5.01C	85	13	2	0	C5.01
2.5Mo-5.0C	84.5	13	2.5	0	C5.0
2.5Mo-5.3C	84.5	13	2.5	0.3	C5.3
2.5Mo-5.45C	84.5	13	2.5	0.45	C5.45
2.5Mo-5.75C	84.5	13	2.5	0.75	C5.75
2.5Mo-6.1C	84.5	13	2.5	1.1	C6.1

The raw materials were ball-milled for 24 h in air atmosphere by adding alcohol. The purpose of ball milling is mainly to mix the powder evenly. The mass ratio of ball-to-powder was 4:1 and rotational velocity was 240 rpm. After milling, the powders were dried at 70 °C for 5 h in a vacuum and then screened by 80 mesh griddles. Then the particle size of the powder was measured with a laser particle size analyzer (Zhu Hai OMEC Instruments Co., Ltd., Zhuhai, China) as shown in Figure 1d. After ball milling, the size of composite powder containing WC, Co, Mo, and carbon black is similar to the size of WC before ball milling.

Afterward, the powders were pressed into a mold with a diameter of 20 mm under 240 MPa. Finally, they were sintered by a pressureless method. The sintering parameters are as follows. The samples were heated from room temperature to 1000 °C at a rate of 10 °C/min, and then to 1430 °C at a heating rate of 5 °C/min and kept at 1430 °C for 1 h, and later were cooled in furnace. The sintering process is carried out under Ar atmosphere, and the operation process of Ar gas is as follows. A vacuum pump was used to pump down the air from the furnace and Ar gas was aerated to the furnace up to atmosphere pressure, and then draw out the Ar gas. After filling and pumping out Ar gas 5 times, the Ar gas was filled again for sintering under atmosphere pressure. The type of furnace used is the Tubular experimental furnace (GSL-1700X, Hefei Kejing Co., Ltd., Hefei, China).

The phase identification of WC-Co and Mo/C-doped WC-Co alloys was measured using XRD-7000 (Shimadzu Co., Ltd., Japan, Cu target). During XRD image analysis, the scanning speed is 5°/min and the scanning angle is 20°–80°. The microstructure was observed by Quanta 250FEG SEM (Czech FEI Co., Ltd., Czech Republic) and the grain size was determined by the software of Image-Pro Plus. Vickers hardness tester was selected to estimate the hardness of alloys. When testing the hardness, the loading force used is 30 kg, which is applied for 10 s. Based on the indentation of Vickers hardness, the total length of indentation crack was obtained to calculate the fracture toughness of alloys (K_{IC} : MPa·m^{1/2}). The etching agent for observing the optical microstructure is the mixed 10% potassium hydroxide solution with 10% potassium ferricyanide, and the etching method is to drop the etching agent onto the degreased cotton and then gently wipe the sample with the degreased cotton. X-ray photoelectron spectroscopy (XPS, Model Axis Supra, Shimadzu-Kratos Analytical Ltd., Manchester, UK) data were measured by monochromatized Al K α X-ray radiation (1486.6 eV).

3. Results and Discussion

3.1. Microstructure and Composition

The XRD patterns of WC-13Co cemented carbide with different Mo and C contents were shown in Figure 2. When the Mo element is added, WC hard phase, Co binder phase, and eta phases were identified in each sample as shown in Figure 2a. The relative intensity of the eta phase diffraction peak enhances with the increase of the Mo content. The WC-Co binary phase diagram indicates that two eta phases are present in the WC-Co system in the low-carbon content, namely, M₆C and M₁₂C [12], which are also named Co₃W₃C and Co₆W₆C [13]. The eta phases form in the sintering process [14]. Among them, the M₆C phase is the high-temperature phase and exists above 1150 °C. With the fall in temperature, it starts to transform into the M₁₂C phase. The M₆C and M₁₂C type carbides have similar FCC crystal structures [15]. In Figure 2b, an interesting phenomenon is that the Mo₂C phase becomes detectable in the samples added Mo and carbon black, accompanied by the decrease of the eta phase. Liu et al. [16] reported that the Mo₂C phase can form below 900 °C when Mo is added to cemented carbide with a high carbon content. The reaction of Mo with carbon black weakened the effect of Mo on the promotion of the eta phase.

Based on the XRD data, the lattice constants were further calculated, as shown in Table 2. It can be seen that the lattice constants of the WC and eta phases did not change significantly when 0%–2.5% Mo was added to the WC-13Co cemented carbide and 0%–1.1% C was added to the WC-13Co-2.5Mo cemented carbide, which indicates that the addition of Mo and C does not cause large lattice strain. Mo and W have very similar atomic radii

(W: 1.37 Å, Mo: 1.36 Å) [17], thus Mo in the place of W will not produce a large lattice strain.

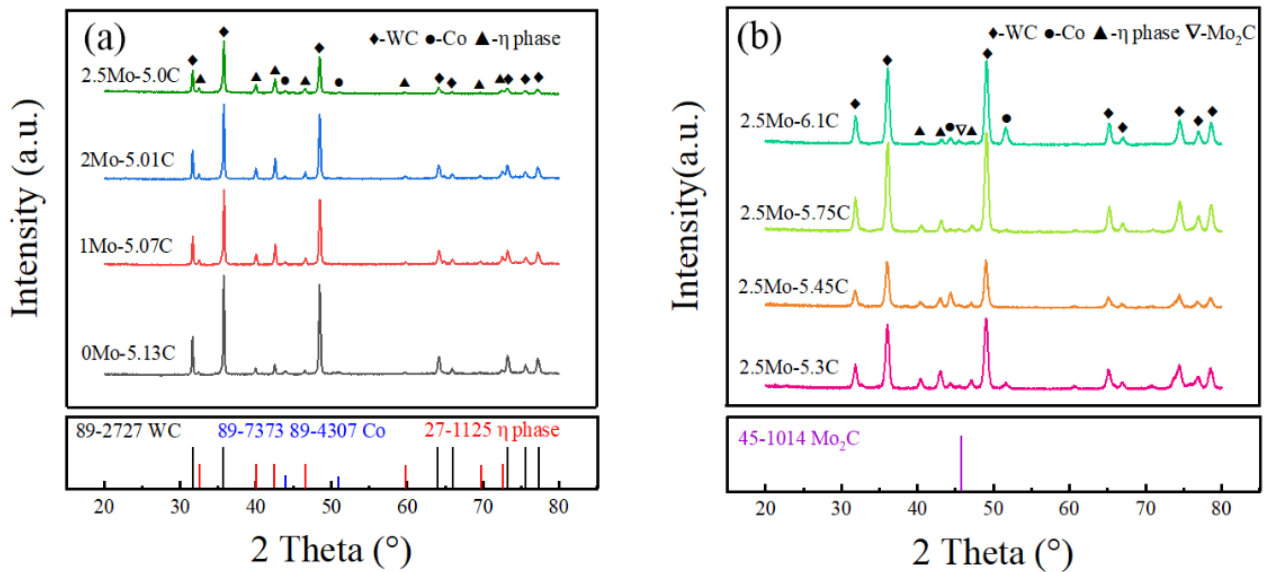


Figure 2. XRD results of WC-13Co alloys with different contents of Mo and C, (a) WC-13Co-x%Mo, (b) WC-13Co-2.5Mo-x%C.

Table 2. Lattice constants of WC and eta phase of various compositions.

Component	WC		Eta Phase a = b = c
	a	b	
0Mo-5.13C	2.90511	2.83594	11.06816
1Mo-5.07C	2.90568	2.83645	11.06775
2Mo-5.01C	2.90464	2.83501	11.05768
2.5Mo-5.0C	2.90543	2.83578	11.06578
2.5Mo-5.3C	2.90644	2.83722	11.05969
2.5Mo-5.45C	2.90599	2.83707	11.0609
2.5Mo-5.75C	2.90453	2.83563	11.03769
2.5Mo-6.1C	2.90495	2.83613	11.03866

Figure 3 illustrates the optical microstructure and Figure 4 further demonstrates the statistical area fraction of the eta phase. The black region in Figure 3 is the corroded eta phase. It is worth noting that the eta phase is very sensitive to the Mo addition. When 2.5% Mo was used to replace WC, the content of C in the alloy decreased by 0.13, and the proportion of the eta phase doubled, from 19.5% to 40%. However, the proportion of the eta phase only decreased from 40% to 34.2% when the addition of carbon black increased from 0 to 0.3%. According to the calculated phase diagram, the ratio of the eta phase should be close to zero for the WC-13Co with a composition of 0Mo-5.13C, and the formation of a large area fraction of the eta phase in Figure 3a is mainly caused by the loss of carbon during sintering [18]. When the content of carbon black reaches 1.1%, the proportion of the eta phase decreases to 4%. Carbon black effectively inhibits the formation of the eta phase in the sample of 2.5Mo-6.1C.

In the WC-Co phase diagram, low-carbon content is the main reason for the formation of the eta phase. The eta phase was also successfully eliminated by increasing the carbon content when producing the inhomogeneous cemented carbides with fine-grained structure via one-step transformation using coarse WC, WO_3 , C, and Co as raw materials by Tang et al. [19].

The eta phase can be clearly observed in the BSE-SEM images as shown in Figure 5. With the addition of Mo from 0% to 2.0%, both the area fraction and the size of the eta phase increase sharply. In the 0Mo-5.13C sample, the eta phase size is relatively small, and most eta phases are slightly larger than WC grains, but in the samples with 2.0% Mo and 2.5% Mo, the size of some eta phases reaches about 10 μm , almost ten times higher than the size of WC grains. With the increase of carbon black in the sample with 2.5% Mo, the large size eta phase disappeared.

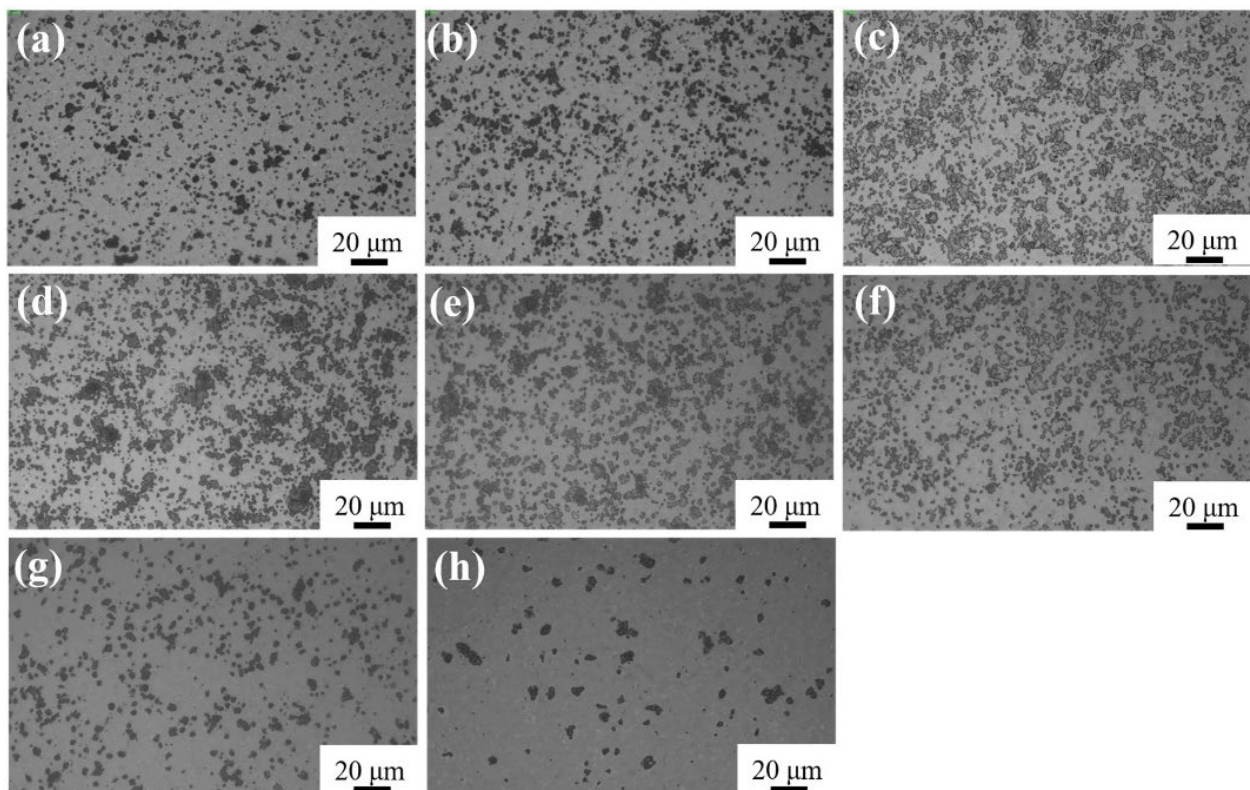


Figure 3. Optical microstructure of WC-13Co with different contents of Mo and C, (a) 0Mo-5.13C, (b) 1Mo-5.07C, (c) 2Mo-5.01C, (d) 2.5Mo-5.0C, (e) 2.5Mo-5.3C, (f) 2.5Mo-5.45C, (g) 2.5Mo-5.75C, (h) 2.5Mo-6.1C.

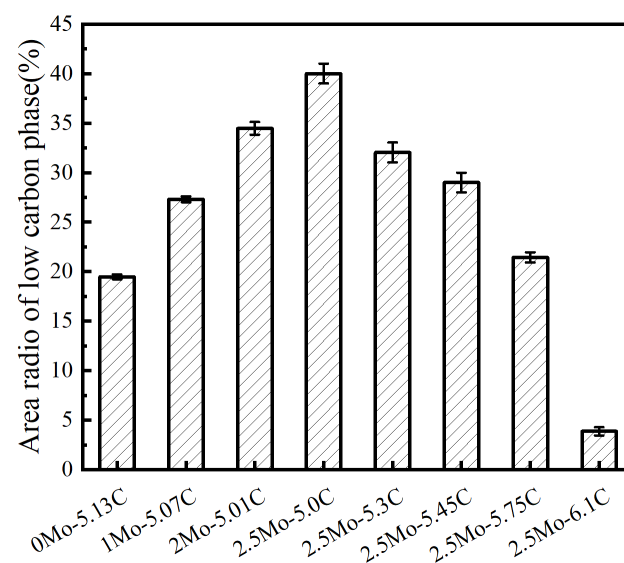


Figure 4. Area fraction of eta phase of WC-13Co with different additions of Mo and C.

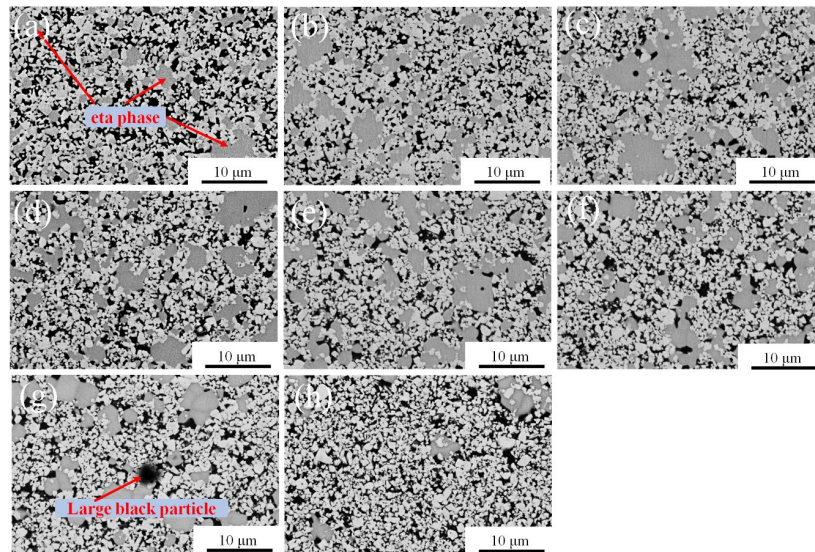


Figure 5. BSE-SEM microstructure of alloys, (a) 0Mo-5.13C, (b) 1Mo-5.07C, (c) 2Mo-5.01C, (d) 2.5Mo-5.0C, (e) 2.5Mo-5.3C, (f) 2.5Mo-5.45C, (g) 2.5Mo-5.75C, (h) 2.5Mo-6.1C.

The distribution of WC grains is shown in Figure 6. As Mo content increases from 0 to 2.5%, WC grain size decreases from ~0.85 to ~0.73 μm. It is well known that the growth and coarsening of WC grains are caused by the Ostwald rippling mechanism. The addition of molybdenum can reduce the solubility of WC in the liquid phase, thus preventing the growth of WC in the liquid phase [20]. Furthermore, Mo precipitates on WC particles, leading to the formation of (W, Mo) C solid solution [16], which slows down the dissolution of WC in the liquid phase, thus inhibiting the dissolution and growth of WC particles.

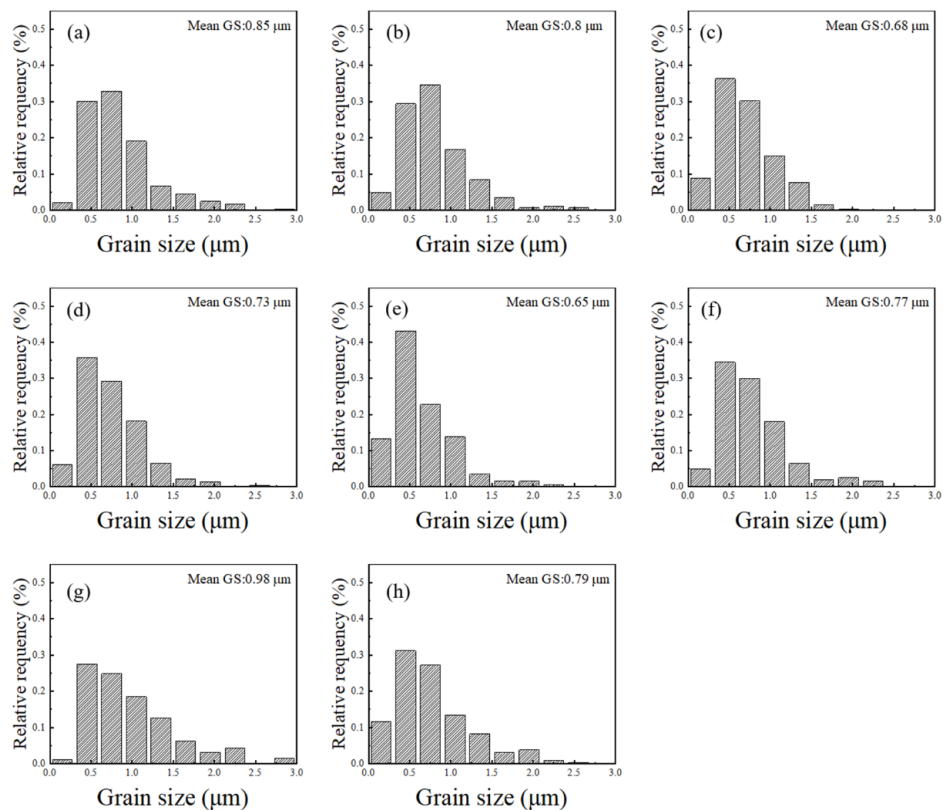


Figure 6. The grain size distribution in WC-13Co with different additions of Mo and C, (a) 0Mo-5.13C, (b) 1Mo-5.07C, (c) 2Mo-5.01C, (d) 2.5Mo-5.0C, (e) 2.5Mo-5.3C, (f) 2.5Mo-5.45C, (g) 2.5Mo-5.75C, (h) 2.5Mo-6.1C.

In contrast, with the increase of carbon black content from 0 to 0.75%, the WC grain size increases from $\sim 0.73 \mu\text{m}$ to $\sim 0.98 \mu\text{m}$. High-carbon content can promote the WC coarsening [21], but with the further increase of carbon black to 1.1%, the WC grain size decreases to $\sim 0.79 \mu\text{m}$. Wei et al. [22] also observed a similar phenomenon, which can be explained by the existence of free carbon in the high-carbon content. The free carbon hinders the solid solution of W and C atoms in the Co phase during liquid phase sintering, which is beneficial to suppress the coarsening of grains during sintering.

The eta phase in the 2.5Mo-5.0C sample was further analyzed by EDS as exhibited in Figures 7 and 8. Surprisingly, it is in the eta phase that the Mo element is mainly enriched in the 2.5Mo-5.0C sample as shown in Figures 7b and 8b. The black binder phase is mainly composed of the Co and W elements. Therefore, in the process route of preparing WC-13Co cemented carbide by powder metallurgy with WC and Co powders as raw materials, when Mo powder is contained in the raw materials, Mo is mainly concentrated in the eta phase if sintering in low-carbon content.

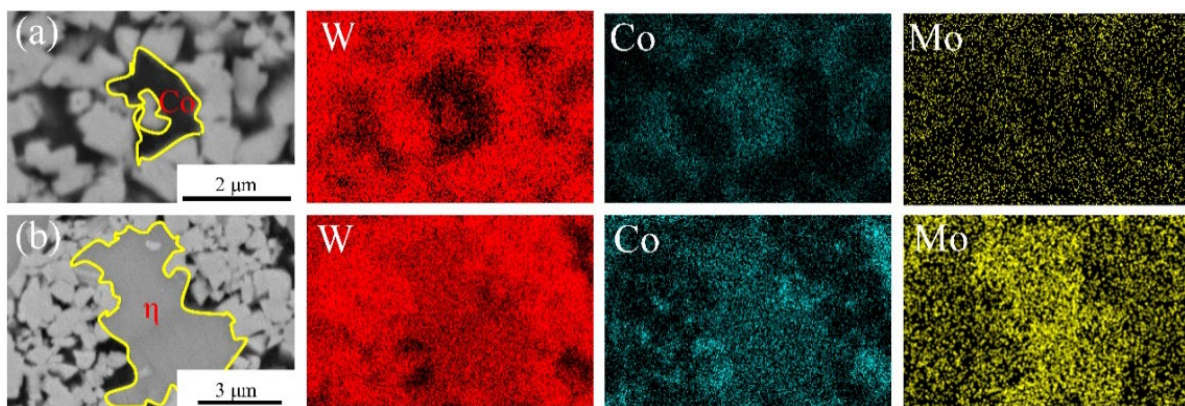


Figure 7. Mapping of elements distribution of the 2.5Mo-5.0C sample. (a) Co phase and (b) eta phase.

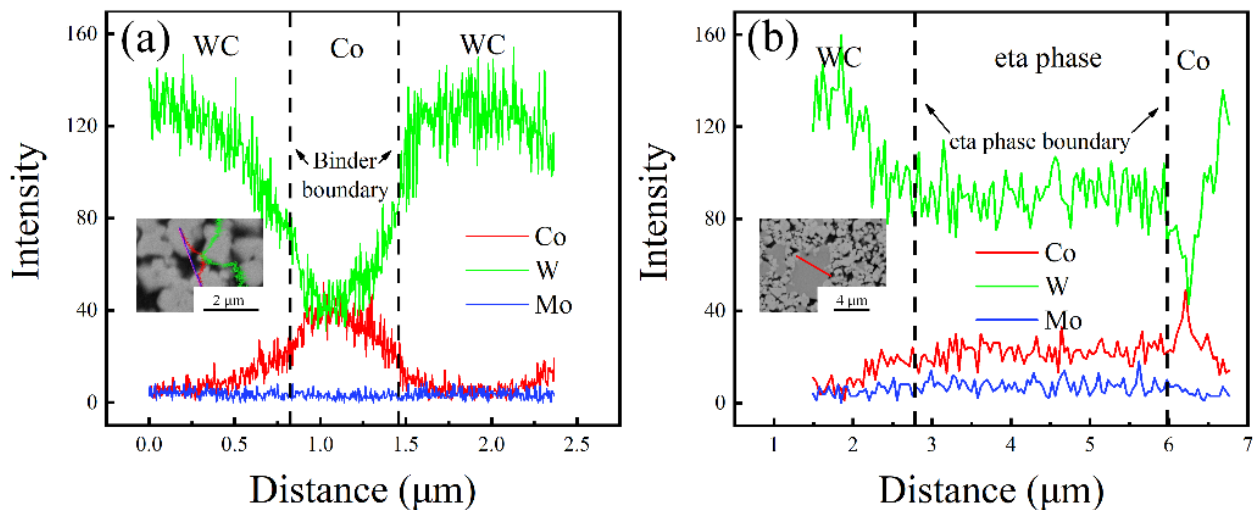


Figure 8. Elements distribution of (a) Co phase and (b) eta phase in the 2.5Mo-5.0C sample.

It is worth noting that some large black particles are observed in Figure 5g. Its composition was analyzed by EDS in Figure 9. The results show that this large particle is enriched with Mo and C. According to the X-ray analysis in Figure 2, this large black particle should be the Mo_2C . It can be seen from Figure 5 that such large spherical particles are a low-frequency occurrence. Guo [7] observed that a small-sized Mo_2C phase forms by the reaction of Mo and C at about 900°C during the sintering process of WC-6Co alloys. Figure 9 also indicates that a large amount of Mo is enriched in the eta phase in the

2.5Mo-5.75C sample, which is consistent with the observation results of the eta phase of the 2.5Mo-5.0C sample as shown in Figures 7 and 8.

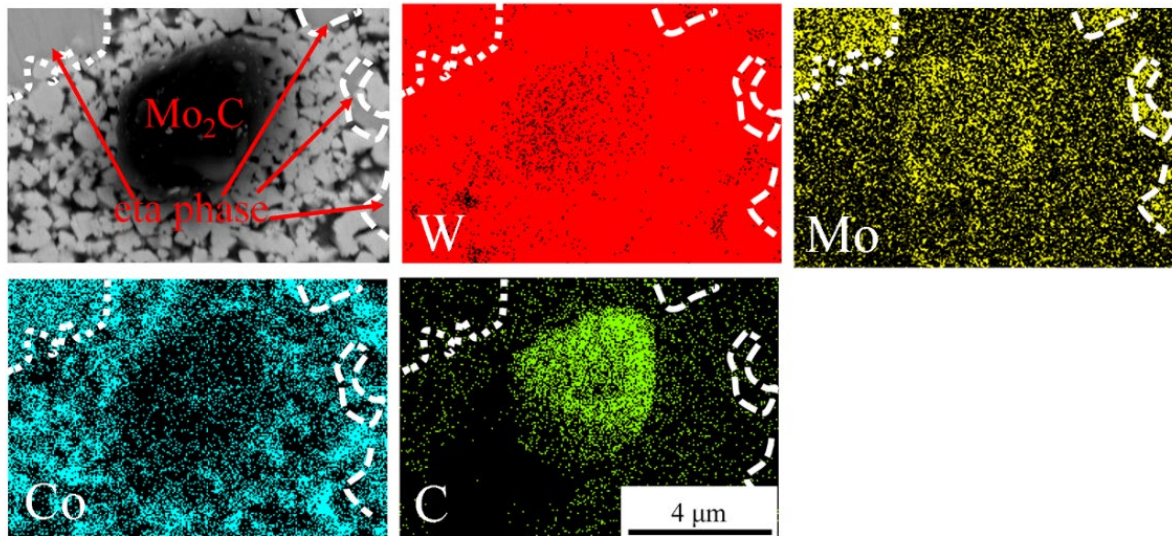


Figure 9. Mapping of element distribution of the 2.5Mo-5.75C sample.

Figure 10 compares the Mo $3d_{3/2}$ and Mo $3d_{5/2}$ XPS spectra of 2.5Mo-5.0C and 2.5Mo-6.1C samples. The main peak of the 2.5Mo-5.0C sample is characterized by Mo $3d_{3/2}$ and Mo $3d_{5/2}$ features at 228.43 and 232.56 eV, while the main peak of 2.5Mo-6.1C sample is characterized by Mo²⁺ $3d_{3/2}$ and Mo²⁺ $3d_{5/2}$ features at 228.05 [23] and 231.27 eV [24] and [25]. Based on the data of XPS, the percentage content of Mo with different valence states was estimated. The fraction of Mo²⁺ and Mo is about 69% and 31% in the 2.5Mo-6.1C sample. Considering the XRD analysis in Figure 2, Mo²⁺ mainly exists in Mo₂C. It should be pointed out that it is useful to estimate the approximate proportion of these atoms and ions according to the statistical theory, although this estimation cannot accurately describe the percentage content of Mo²⁺ and Mo.

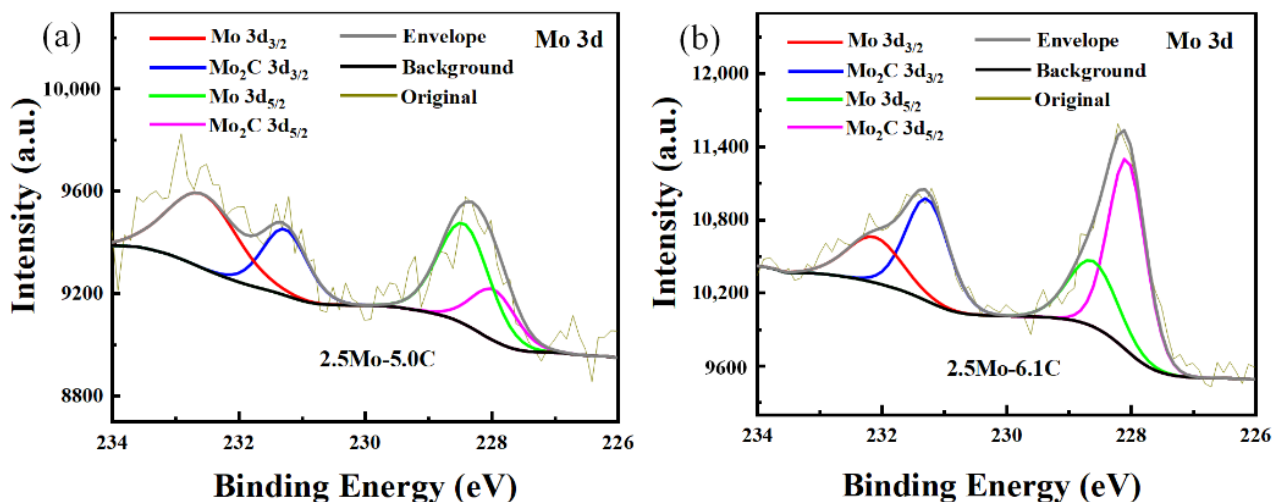


Figure 10. XPS survey spectra of 2.5Mo-5.0C (a) and 2.5Mo-6.1C (b) samples.

To sum up, when Mo is added to WC-Co cemented carbide, the content of C determines its existing state. In low-carbon contents, Mo is mainly distributed in the eta phase, partially replacing the positions of W and Co atoms. When the eta phase is formed, Mo can infinitely replace W, forming an infinite solid solution and Mo is not observed in the Co binder phase. According to the reports [17], the radius of W and Mo atomic is very close (W: 1.37 Å,

Mo: 1.36 Å). In a high-carbon environment, the Mo element preferentially exists in Mo_2C , and a small amount of Mo appears in the eta phase partially replacing the lattice position of W and Co.

3.2. Mechanical Properties

Figure 11 illustrates the hardness and fracture toughness of all samples. The alloy without adding Mo has the lowest hardness value. When the Mo content increases from 0 to 2.5%, the eta phase grows abnormally and the area fraction of the eta phase significantly increases to 40%, leading to an obvious increase in hardness from 1232 HV₃₀ to 1321 HV₃₀, and the decrease in fracture toughness from 12.5 MPa·m^{1/2} to 9.8 MPa·m^{1/2}. This is different from the experimental results of Wang [20]. They found that the increase of Mo improved the fracture toughness because Mo slows down the transformation from FCC-Co to HCP-Co. From Figures 5, 7 and 8, it is deduced that Mo is mainly concentrated in the eta phase in the samples of 0Mo-5.13C, 1Mo-5.07C, 2Mo-5.01C, and 2.5Mo-5.0C. The appearance of a large-sized eta phase is harmful to fracture toughness.

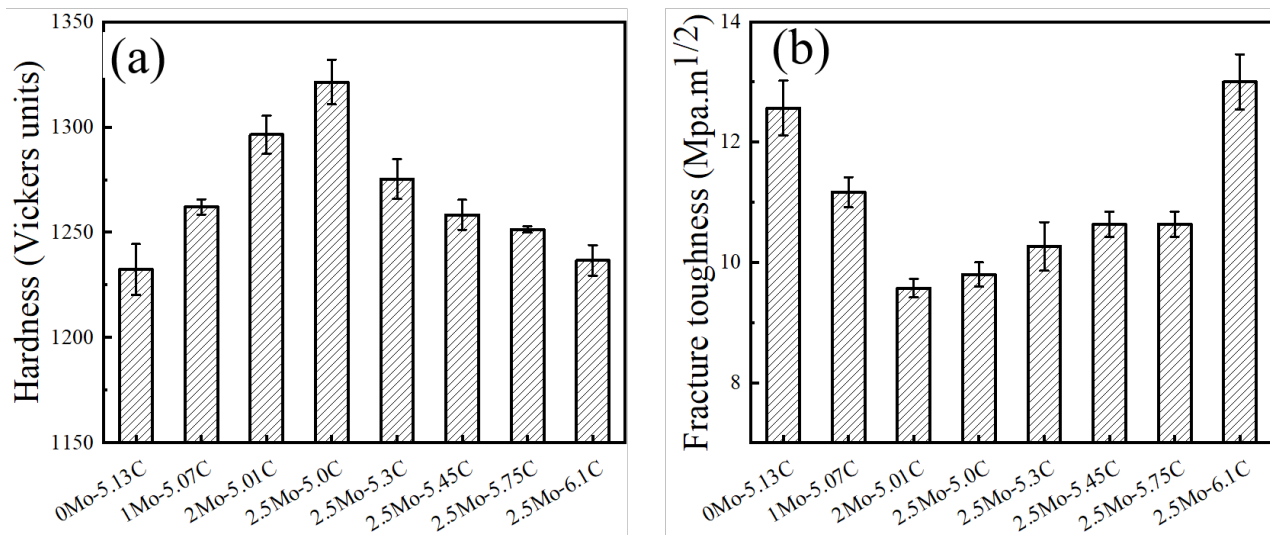


Figure 11. The hardness (a) and fracture toughness of different cemented carbides (b).

After adding carbon black to samples with 2.5% Mo added, the eta phase was restrained. Compared with the fracture toughness of 9.8 MPa·m^{1/2} in the 2.5Mo-5.0C sample without adding carbon black, the fracture toughness of the 2.5Mo-6.1C sample increased by about 32%. The fracture toughness and hardness of the 2.5Mo-6.1C sample are slightly higher than those of the 0Mo-5.13C sample, which is very important to the preparation of WC-Co cemented carbide containing Mo for improving the corrosion resistance.

The hardness of WC-Co cemented carbides is strongly dependent on the content of the Co binder [26], the grain size of WC, and the eta phase [27]. The eta phase enhances the WC-Co but decreases the toughness. After the addition of 1%, 2%, or 2.5% Mo, a large amount of Co reacts and converts to the eta phase, which leads to the decrease of the Co binder phase, the decrease of grain size (Figure 6), and the increase of eta (Figures 4 and 5). All of these factors lead to the increase in the hardness of the cemented carbide. Therefore, the hardness increases with the increase of Mo content in Figure 11. However, after adding carbon black, the content of the eta phase decreases, the content of the Co binder increases, the grain size increases, and the hardness decreases. It should be noted that the sample of 2.5Mo-6.1C also has a small grain size, but its hardness is low, which is mainly due to the large reduction of the eta phase and the increase of the proportion of the Co binder phase. The fracture toughness of WC-Co cemented carbides is chiefly affected by the free path of the Co binder phase [28]. It can be seen from Figure 5 that the distribution of the Co phase is relatively uniform, thus the higher the content of the Co phase, the better the fracture

toughness. The specimen prepared with the carbon addition of 1.1 wt.% has the lowest content of eta and the highest fracture toughness of $13 \text{ MPa}\cdot\text{m}^{1/2}$.

Figure 12 demonstrates crack propagation in 0Mo-5.13C and 2.5Mo-5.0C, which have higher and lower fracture toughness, respectively. The length of the crack affects the calculation of the value of fracture toughness. In Figure 12a, the type of crack propagation includes intergranular and transgranular fractures [29]. More cracks in the 0Mo-5.13C sample are extended between WC particles, while the large-sized eta phase in the 2.5Mo-5.0C sample leads to the formation of long flat transgranular cracks as shown in Figure 12b, which significantly reduces the fracture toughness [30].

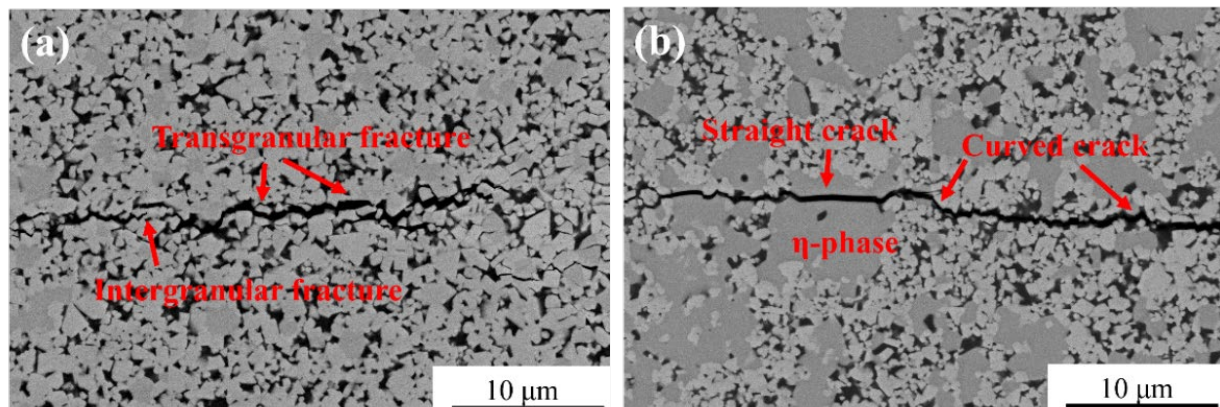


Figure 12. Crack microstructure of (a) 0Mo-5.13C, and (b) 2.5Mo-5.0C samples.

3.3. Influence Mechanism of the Addition of Mo

According to the Ostwald ripening mechanism, WC grains will grow gradually due to the dynamic balance of dissolution and precipitation of WC in the Co binder phase when WC-Co cemented carbide is prepared by liquid phase sintering. Wang et al. [20] pointed out that the addition of Mo precipitates on the surface of WC grains, thus hindering the growth of WC grains and resulting in the refinement of the WC grains of sintering WC-Co cemented carbides. In this study, it is found that Mo has more influence on the development of the phases in both low-carbon and high-carbon contents. In low-carbon content, Mo mainly concentrates in the eta phase, as shown in Figures 5 and 7, and Mo significantly promotes the development of the eta phase. In a high-carbon environment, Mo mainly exists in the Mo_2C phase, as shown in Figures 2 and 10. In contrast, the addition of Mo has relatively less effect on the size of WC grains.

Moreover, Guo et al. [7] reported on the small-sized Mo_2C formed by the reaction between Mo and C in WC-Co alloys, and that most of them are distributed in the Co binder phase. Different from the reports, it is observed in Figure 9 that some Mo_2C particles with larger sizes above $3 \mu\text{m}$ form by the reaction of Mo and C, although the number of large-sized Mo_2C particles is very small. It is inferred that the reduction of the size of Mo powder in raw materials is helpful to eliminate the large-sized Mo_2C particle.

Based on the above analysis, Figure 13 illustrates the reaction diagram in the heating process of sintering: (i) for the Composition Design I without adding Mo, the alloy is composed of the WC grain, the Co binder, and eta phase after sintering in the low-carbon contents; (ii) for the Composition Design II of adding Mo powder in the sample with low-carbon content, the eta phase of $[\text{W}, \text{Co}, \text{Mo}] \text{C}$ forms by the reaction of Mo, Co, and WC when the temperature rises to $900\text{--}1100 \text{ }^\circ\text{C}$, and Mo mainly concentrates in the eta phases; (iii) for the Composition Design III of adding Mo powder and sintering in a high-carbon environment, the Mo_2C preferentially forms by the reaction of Mo and C at $900\text{--}1100 \text{ }^\circ\text{C}$ and the remaining part of Mo mainly exists in the eta phase of $[\text{W}, \text{Co}, \text{Mo}] \text{C}$ after sintering.

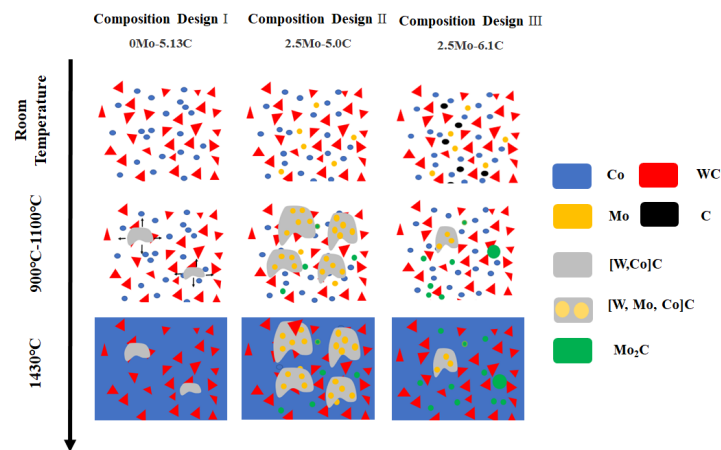


Figure 13. The reaction diagram in the heating process of sintering in WC-Co cemented carbides adding different contents of Mo and C.

4. Conclusions

The addition of Mo in WC-13Co cemented carbides has an obvious impact on the composition, size, and distribution of the eta phase and Mo_2C phase, and shows different results in low-carbon and high-carbon contents.

Without the addition of Mo, the eta phase of the WC-13Co cemented carbides is composed of the elements of Co, W, and C. After adding 2.5% Mo in low-carbon contents, the eta phase is composed of Co, W, Mo, and C. With the increase of Mo content from 0 to 2.5% in WC-13Co cemented carbides, the Mo-enriched eta phase grows abnormally and the area fraction of the eta phase significantly increases from 19.4% to 40%, leading to an obvious increase in hardness from 1232 HV_{30} to 1321 HV_{30} , and the decrease in fracture toughness from $12.5 \text{ MPa}\cdot\text{m}^{1/2}$ to $9.8 \text{ MPa}\cdot\text{m}^{1/2}$. With the increase of carbon black content from 0 to 1.1% in WC-13Co-2.5Mo cemented carbides, the formation of the eta phase is inhibited and a small number of large-sized Mo_2C occurs. The fracture toughness clearly increases from $9.8 \text{ MPa}\cdot\text{m}^{1/2}$ to $13 \text{ MPa}\cdot\text{m}^{1/2}$ while the hardness decreases from 1321 HV_{30} to 1237 HV_{30} .

In view of the beneficial effect of Mo addition on mechanical properties and corrosion resistance of WC-Co cemented carbides found in previous reports, it is believed that this work can contribute to the control of the eta phase of WC-Co cemented carbides containing Mo for industrial production.

Author Contributions: Conceptualization, J.L. and V.J.; methodology, J.L. and X.L.; formal analysis, X.L.; investigation, X.L. and X.Z.; resources, X.Z., J.Z. and Q.Z.; writing—original draft preparation, X.L.; writing—review and editing, J.L. All authors have read and agreed to the published version of the manuscript.

Funding: This work was funded by the Fundamental Research Funds for the Central Universities (No. N2002008), and the Science and Technology Plan Project of Shenfu Demonstration District (2021JH05).

Institutional Review Board Statement: Not applicable.

Informed Consent Statement: Not applicable.

Data Availability Statement: Not applicable.

Conflicts of Interest: The authors declare no conflict of interest.

References

- Lu, Z.; Du, J.; Sun, Y.; Su, G.; Zhang, C.; Kong, X. Effect of ultrafine WC contents on the microstructures, mechanical properties and wear resistances of regenerated coarse grained WC-10Co cemented carbides. *Int. J. Refract. Met. Hard Mater.* **2021**, *97*, 105516. [[CrossRef](#)]
- Rayón, E.; Bonache, V.; Salvador, M.D.; Roa, J.J.; Sánchez, E. Hardness and Young's modulus distributions in atmospheric plasma sprayed WC-Co coatings using nanoindentation. *Surf. Coat. Technol.* **2011**, *205*, 4192–4197. [[CrossRef](#)]

3. Li, J.; Cheng, J.; Chen, P.; Chen, W.; Wei, B.; Liu, J. Effects of partial substitution of copper for cobalt on the microstructure and properties of ultrafine-grained WC-Co cemented carbides. *J. Alloys Compd.* **2018**, *735*, 43–50. [[CrossRef](#)]
4. Fazili, A.; Derakhshandeh, M.R.; Nejadshamsi, S.; Nikzad, L.; Razavi, M.; Ghasali, E. Improved electrochemical and mechanical performance of WC-Co cemented carbide by replacing a part of Co with Al₂O₃. *J. Alloys Compd.* **2020**, *823*, 153857. [[CrossRef](#)]
5. Yu, B.; Li, Y.; Lei, Q.; Nie, Y. Microstructures and mechanical properties of WC-Co-xCr-Mo cement carbides. *J. Alloys Compd.* **2019**, *771*, 636–642. [[CrossRef](#)]
6. Lin, N.; Wu, C.H.; He, Y.H.; Zhang, D.F. Effect of Mo and Co additions on the microstructure and properties of WC-TiC-Ni cemented carbides. *Int. J. Refract. Met. Hard Mater.* **2012**, *30*, 107–113. [[CrossRef](#)]
7. Guo, Z.; Xiong, J.; Yang, M.; Song, X.; Jiang, C. Effect of Mo₂C on the microstructure and properties of WC-TiC-Ni alloy. *Int. J. Refract. Met. Hard Mater.* **2008**, *26*, 601–605. [[CrossRef](#)]
8. Genga, R.M.; Cornish, L.A.; Akdogan, G. Effect of Mo₂C additions on the properties of SPS manufactured WC-TiC-Ni alloys. *Int. J. Refract. Met. Hard Mater.* **2013**, *41*, 12–21. [[CrossRef](#)]
9. Lin, Z.; Xiong, J.; Guo, Z.; Zhou, W.; Wan, W.; Yang, L. Effect of Mo₂C addition on the microstructure and fracture behavior of (W, Ti) C-based alloys. *Ceram. Int.* **2014**, *40*, 16421–16428. [[CrossRef](#)]
10. Guo, S.; Bao, R.; Yang, J.; Chen, H.; Yi, J. Effect of Mo and Y₂O₃ additions on the microstructure and properties of fine WC-Co cemented carbides fabricated by spark plasma sintering. *Int. J. Refract. Met. Hard Mater.* **2017**, *69*, 1–10. [[CrossRef](#)]
11. Ban, Z.G.; Shaw, L.L. On the reaction sequence of WC-Co formation using an integrated mechanical and thermal activation process. *Acta Mater.* **2001**, *49*, 2933–2939. [[CrossRef](#)]
12. Guillermet, A.F. Thermodynamic properties of the Co-W-C system. *Metall. Trans. A* **1989**, *20*, 935–956. [[CrossRef](#)]
13. Markström, A.; Frisk, K.; Sundman, B. A revised thermodynamic description of the Co-W-C system. *J. Phase Equilib. Diffus.* **2005**, *26*, 152–160. [[CrossRef](#)]
14. Janusz, L. Positions of the carbon atoms in Fe₆W₆C. *J. Less Common Met.* **1964**, *7*, 318–320.
15. Janisch, D.S.; Garel, M.; Eder, A.; Lengauer, W.; Dreyer, K.; van den Berg, H. Sintering, characterization, and analysis of functional gradient hardmetals. *Int. J. Refract. Met. Hard Mater.* **2008**, *26*, 179–189. [[CrossRef](#)]
16. Liu, N.; Xu, Y.; Li, Z.; Chen, M.; Li, G.; Zhang, L. Influence of molybdenum addition on the microstructure and mechanical properties of TiC-based cermets with nano-TiN modification. *Ceram. Int.* **2003**, *29*, 915–925. [[CrossRef](#)]
17. Zhou, Y.; Lin, Y.; Zhang, F.; Jiang, Y.; Wei, S.; Xu, L.; Chong, X.; Li, Z.; Feng, J. Lattice stability, mechanical and thermal properties of a new class of multicomponent (Fe, Mo, W)₆C η carbides with different atomic site configurations. *Ceram. Int.* **2022**, *48*, 5107–5118. [[CrossRef](#)]
18. Rabouhi, H.; Khelifaoui, Y.; Khireddine, A. Comparative study by image analysis of WC-Co alloys elaborated by liquid phase sintering and hot isostatic pressing. *Int. Inform. Eng. Technol. Assoc.* **2020**, *44*, 263–269. [[CrossRef](#)]
19. Tang, Y.; Wang, S.; Xu, F.; Hong, Y.; Luo, X.; He, S.; Chen, L.; Zhong, Z.; Chen, H.; Xu, G.; et al. Effect of carbon content on the properties of inhomogeneous cemented carbides with fine-grained structures produced via one-step transformation. *J. Alloys Compd.* **2021**, *882*, 160638. [[CrossRef](#)]
20. Wang, Y.; Liu, W.; Zhong, C.; Wu, J.; Ye, Y. Effects of partial substitution of Cu for Co on the microstructure and properties of WC-Co-Mo cemented carbides. *Ceram. Int.* **2021**, *47*, 13519–13527. [[CrossRef](#)]
21. Konyashin, I.; Hlawatschek, S.; Ries, B.; Lachmann, F.; Dorn, F.; Sologubenko, A.; Weirich, T. On the mechanism of WC coarsening in WC-Co hard metals with various carbon contents. *Int. J. Refract. Met. Hard Mater.* **2009**, *27*, 234–243. [[CrossRef](#)]
22. Wei, C.; Song, X.; Fu, J.; Lv, X.; Wang, H.; Gao, Y.; Zhao, S.; Liu, X. Effect of Carbon Addition on Microstructure and Properties of WC-Co Cemented Carbides. *J. Mater. Sci. Technol.* **2012**, *28*, 837–843. [[CrossRef](#)]
23. Perret, N.; Wang, X.; Delannoy, L.; Potvin, C.; Louis, C.; Keane, M.A. Enhanced selective nitroarene hydrogenation over Au supported on β-Mo₂C and β-Mo₂C/Al₂O₃. *J. Catal.* **2012**, *286*, 172–183. [[CrossRef](#)]
24. Weigert, E.C.; Esposito, D.V.; Chen, J.G. Cyclic voltammetry and X-ray photoelectron spectroscopy studies of electrochemical stability of clean and Pt-modified tungsten and molybdenum carbide (WC and Mo₂C) electrocatalysts. *J. Power Sources* **2009**, *193*, 501–506. [[CrossRef](#)]
25. Hara, Y.; Minami, N.; Itagaki, H. Synthesis and characterization of high-surface area tungsten carbides and application to electrocatalytic hydrogen oxidation. *Appl. Catal. A-Gen.* **2007**, *323*, 86–93. [[CrossRef](#)]
26. Tabrizi, A.T.; Pouzesh, M.; Laleh, F.F.; Aghajani, H. Evaluation of the corrosion resistance of WC-Co coating on AZ91 applied by electro spark deposition. *Powder Metall. Prog.* **2020**, *20*, 30–40. [[CrossRef](#)]
27. Da Costa, F.A.; De Medeiros, F.F.P.; Da Silva, A.G.P.; Gomes, U.U.; Filgueira, M.; De Souza, C.P. Structure and hardness of a hard metal alloy prepared with a WC powder synthesized at low temperature. *Mater. Sci. Eng. A* **2008**, *485*, 638–642. [[CrossRef](#)]
28. Fang, Z.; Griffo, A.; White, B.; Lockwood, G.; Belnap, D.; Hilmas, G.; Bitler, J. Fracture resistant super hard materials and hardmetals composite with functionally designed microstructure. *Int. J. Refract. Met. Hard Mater.* **2001**, *19*, 453–459. [[CrossRef](#)]
29. Chang, S.H.; Chang, M.H.; Huang, K.T. Study on the sintered characteristics and properties of nanostructured WC-15 wt.% (Fe-Ni-Co) and WC-15 wt.% Co hard metal alloys. *J. Alloys Compd.* **2015**, *649*, 89–95. [[CrossRef](#)]
30. Pristiniski, Y.; Peretyagin, N. Comparative studies on mechanical properties of WC-Co composites sintered by SPS and conventional techniques. *MATEC Web Conf.* **2017**, *129*, 02028. [[CrossRef](#)]